IAC-23-A6.2.6

Large-scale mapping and analysis of collision avoidance manoeuvres with semi-analytical models

Juan Luis Gonzalo[a]*, Manuel Sanjurjo Rivo[b], Camilla Colombo[a]

[a] *Department of Aerospace Science and Technology, Politecnico di Milano, Via la Masa 34, Milan 20156, Italy,* juanluis.gonzalo@polimi.it
[b] *Universidad Carlos III de Madrid, Avenida Universidad 30, Leganés 28911, Spain*
* Corresponding Author

Abstract

The continuous increase in space traffic and the accumulation of space debris causes a growing stress on space traffic management and space situational awareness systems. Regarding collision avoidance activities, recent advancements to cope with the increasing number of close approaches (CAs) focus on introducing a higher level of autonomy (either for ground operations or on-board), managing large constellations, updating the tools and models to account for the adoption of low-thrust propulsion, and improving the characterization of uncertainties, among others. In many of these cases, large-scale simulations are required to train, inform, or validate the models, which can be a challenge particularly in low-thrust scenarios.

This work presents a sensitivity analysis of collision avoidance manoeuvres (CAMs) in different operational scenarios both for impulsive and low-thrust propulsion systems. These analyses are enabled by the high-performance analytic and semi-analytic models in the MISS (Manoeuvre Intelligence for Space Safety) framework developed at Politecnico di Milano. The different models are based on the single-averaging of the equations of motion, formulated in Keplerian elements. For the low-thrust case, arbitrary thrust directions are managed through the superposition of solutions for the tangential and normal directions. Both for impulsive and low-thrust CAMs, manoeuvre design methods for miss distance minimization and probability of collision maximization are described. These models are then used to construct maps for a set of representative scenarios. From the analysis of these maps, key conclusions on the CAM's behaviour are drawn. Finally, the use of these maps for applications like training machine learning models is briefly discussed.

Keywords: Collision avoidance manoeuvre, analytical methods, Space Traffic Management, Space Situational Awareness

Nomenclature

a	Semi-major axis, km
$\boldsymbol{a}_T$	Perturbing acceleration vector
a_n	Normal thrust acceleration, km/s^2
a_t	Tangential thrust acceleration, km/s^2
e	Eccentricity
E	Eccentric anomaly, deg or rad
n	Mean motion of the spacecraft, 1/s
r	Orbital radius, km
t	Time, s
v	Orbital velocity (magnitude), km/s
$\boldsymbol{\alpha}$	Vector of Keplerian elements
Δt	Impulsive CAM lead time, s
ε	Non-dimensional thrust parameter
μ	Gravitational parameter of the primary, km^3/s^2
ω	Argument of pericentre, deg or rad
Ω	Right ascension of the ascending node, deg or rad

Acronyms/Abbreviations

CA	Close approach
CAM	Collision avoidance manoeuvre
COLA	Collision Avoidance
PoC	Probability of Collision
ref	Reference value
TCA	Time of closest approach

1. Introduction

The continuous increase in space traffic and the accumulation of space debris means a growing stress on space traffic management (STM) and space situational awareness systems. This is a multi-faceted challenge, requiring sustained advances in a diverse set of fields like space surveillance and tracking, policy and regulations, debris mitigation, and collision avoidance (COLA). For what regards COLA activities, recent developments have focused on dealing with the increasing number of close approaches (CAs) by introducing a higher level of autonomy through artificial intelligence (either to assist ground operations or introduce on-board capabilities), the challenge of managing large constellations, updating the tools and models to account for the adoption of low-thrust propulsion, and improving the characterization of uncertainties, among other topics. In many of these cases, large-scale simulations are required to train, inform, or validate the models, which can be a challenge particularly in low-thrust scenarios.

A key challenge when performing large-scale simulations for the analysis and design of collision avoidance manoeuvres (CAMs) are the associated computational costs. This problem is particularly relevant for low thrust spacecraft, where fully numerical methods require the formulation and resolution of an optimal control problem, typically in an iterative manner. To tackle this limitation, several authors have proposed approximate analytical and semi-analytical models for impulsive [1] and low-thrust CAMs [2]. These models provide computationally efficient and algorithmically robust solutions, while they present limitations in terms of the perturbation models that can be included, the introduction of operational constraints, and the accuracy of the solution.

The case of low thrust CAM is particularly challenging, for different reasons. On the one hand, the smaller control authority implies longer manoeuvre times and reduced reachability domains, adding complexity to the CAM design and operational restrictions on the CAM planning and decision to act by ground operators. Furthermore, the longer thrust arcs and the noise in thrust can affect the evolution of uncertainties. Acknowledging these challenges, the European Space Agency funded the ELECTROCAM project, which was recently completed, to advance their models and tools for the analysis of low thrust COLA activities. The project covers several aspects, including the assessment of current capabilities of low thrust satellites [3], propagation of uncertainties[4][5], efficient analytical and semi-analytical models for CAMs [6], and update of ESA's operational software tool ARES. The low thrust CAM models that are considered in this work have been partially developed within the ELECTROCAM project.

This work focuses on the use of highly-efficient analytical and semi-analytical CAM models for mapping the effect on the CAM of different parameters, such as the thrust level, the timing of the CAM, and the evolution of uncertainties. Different operational scenarios are considered, both for impulsive and low-thrust propulsion systems. This large-scale mapping is enabled by the high-performance analytic and semi-analytic models in the MISS (Manoeuvre Intelligence for Space Safety) set of algorithms developed by Politecnico di Milano [7]. These models rely on the single-averaging of the equations of motion expressed in Keplerian elements; while this is straightforward for the impulsive case [8], more elaborate expression are reached for low-thrust CAMs [9][10]. In this case, scenarios with arbitrary thrust directions are managed through the superposition of solutions for the tangential and normal directions [11], whose solutions are obtained in terms of complete elliptic integrals and series expansions of the reference eccentricity. Both for impulsive and low-thrust CAMs, manoeuvre design methods for miss distance minimization and probability of collision maximization are also defined.

The rest of this document is organized as follows. First, the problem at hand is defined, and the mathematical models are briefly introduced. The detailed derivation of the models can be found in previous works by the authors, and is omitted for brevity. Then, these models are used to construct maps of solutions for different scenarios. From the analysis of these maps, key conclusions on the CAM's behaviour are drawn. Finally, the use of these solutions for applications like machine learning models training or surrogate model design for on-board applications is briefly discussed.

2. Collision avoidance problem statement

Let us consider a predicted CA between a manoeuvrable spacecraft and a non-cooperative object at a nominal time of closest approach TCA. The term non-cooperative object is used here in a generic way to refer to any orbiting object that cannot, or will not, act in response to the CA; e.g., a debris, a spacecraft without manoeuvring capabilities, or a spacecraft whose operator decides not to act. The orbit determination process for both objects is subjected to uncertainties, characterized by their respective covariance matrices. In the following, it is assumed that the CA corresponds to a short-term encounter, and that the covariance matrices of both objects are statistically independent. This allows us to restrict the CA analysis to the encounter plane (i.e., the plane perpendicular to the relative velocity at TCA), and to simplify the problem by considering a debris with no volume and the combined uncertainty of both objects, and a spacecraft with no uncertainty and the combined hard body radius of both objects.

The manoeuvrable spacecraft is equipped with either an impulsive or a low-thrust propulsion system. The goal of the CAM is to increase the miss distance and reduce the PoC to acceptable levels, while minimizing the disruption to the nominal orbit. In this sense, it is assumed that the deviation from the nominal orbit is small, allowing for the use of linearized relative motion models.

The mathematical models describing the CAM, both for the impulsive and low-thrust cases, are summarized in Section 3.

3. Analytical and semi-analytical CAM models

The proposed (semi-)analytical CAM framework relies on the assumption that the displacement due to the CAM is small, allowing to characterize the post-manoeuvre orbit through the modification $\delta\boldsymbol{\alpha}$ of its Keplerian state $\boldsymbol{\alpha} = [a, e, i, \Omega, \omega, M]^T$, and to map changes in Keplerian state to displacements $\delta\boldsymbol{r}$ at TCA using linearized relative motion models [12]. This $\delta\boldsymbol{r}$ at TCA (or more generally, $\delta\boldsymbol{s} = [\delta\boldsymbol{r}^T\ \delta\boldsymbol{v}^T]^T$) is then projected on the nominal encounter plane, or b-plane, to characterize the updated CA in terms of miss distance and PoC. This workflow is depicted in Fig. 1.

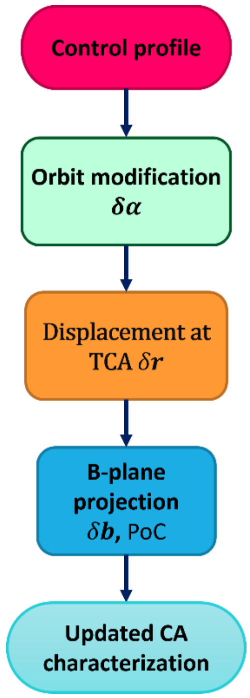

Fig. 1. Conceptual structure of the (semi-)analytical CAM models

The procedure is configured in a modular way [7], where the second and third blocks, displacement at TCA and b-plane projection, respectively, are independent of the orbit modification model and can be applied both to the impulsive and low-thrust cases. In the most general case, the mapping from $\delta\boldsymbol{\alpha}$ to changes in position and velocity at TCA can be expressed as [12]:

$$\begin{bmatrix}\delta\boldsymbol{r}\\ \delta\boldsymbol{v}\end{bmatrix}(TCA) = \begin{bmatrix}\boldsymbol{A}_r\\ \boldsymbol{A}_v\end{bmatrix}\delta\boldsymbol{\alpha}(TCA) \tag{1}$$

where $\boldsymbol{A}_r$ and $\boldsymbol{A}_v$ are 3×6 matrices that depend only on the nominal orbit [8]. On the other hand, the displacement in the b-plane is directly computed from the projection of $\delta\boldsymbol{r}$ onto this plane, and the PoC is evaluated using Chan's algorithm [13] both for computational efficiency and for ease of analytical manipulation.

The model for the change in Keplerian elements, instead, is strongly dependent on the type of CAM considered. In the following two subsections, the models for the impulsive and the low-thrust case are briefly introduced. In both cases, they are based on Gauss's planetary equations, which can be expressed in linear form as [14]:

$$\frac{\mathrm{d}\boldsymbol{\alpha}}{\mathrm{d}t} = \boldsymbol{G}(\boldsymbol{\alpha}, t)\ \boldsymbol{a}_T \tag{2}$$

3.1 Impulsive CAM

For the impulsive CAM, a matrix relation between the manoeuvre delta-V and the instantaneous change in Keplerian elements is obtained by integrating Eq. (2) over the instantaneous duration of the manoeuvre [8]. However, as noted in [15] for the case of asteroid deflection, an additional correction in the mean anomaly is needed to account for the change in mean motion during the manoeuvre lead time $\Delta t = TCA - t_{CAM}$. Both contributions can be combined in a single matrix expression:

$$\delta\boldsymbol{\alpha}\,(TCA) = \boldsymbol{G}^I(\boldsymbol{\alpha}, t_{CAM}, \Delta t)\delta\boldsymbol{v}\,(t_{CAM}) \tag{3}$$

Combining Eqs. (2) and (3), a linear mapping between $\delta\boldsymbol{v}\,(t_{CAM})$ and $\delta\boldsymbol{r}(TCA)$ is reached. This can be leveraged to reduce the miss distance maximization problem to an eigenproblem, as noted by Conway for a different application of asteroid deflection [17]. In a later work, Bombardelli and Hernando-Ayuso [1] proved that this approach can also be extended to the PoC minimization problem, introducing the information of the combined covariance into the linear mapping. In both cases, the optimization problem is a quadratic one, and the optimal thrust direction is given by the eigenvector associated to the largest eigenvalue.

3.2 Low-thrust CAM

The derivation of the averaged low-thrust model is significantly more involved than that of the impulsive one. To perform the averaging of the equations of motion, Eq. (2), over one revolution, they must be expressed in terms of a suitable anomaly. We consider the eccentric anomaly E, whose time evolution is given by:

$$\frac{\mathrm{d}E}{\mathrm{d}t} = \boldsymbol{G}_E(\boldsymbol{\alpha}, t)\boldsymbol{a}_T \tag{4}$$

Inverting Eq. (4), a differential time law $\mathrm{d}t/\mathrm{d}E$ is obtained, and from it the ODE system for $\boldsymbol{\alpha}$ as function of E, $\mathrm{d}\boldsymbol{\alpha}/\mathrm{d}E$. However, the expressions are too cumbersome to obtain their analytical average directly. Assuming small thrust acceleration, the evolution of $\boldsymbol{\alpha}$ can be linearized in thrust acceleration to separate the tangential and normal components (denoted by superscripts *t*, *n*, respectively):

$$\boldsymbol{\alpha} = \boldsymbol{\alpha}_{ref} + \varepsilon_t\boldsymbol{\alpha}^t(E) + \varepsilon_n\boldsymbol{\alpha}^n(E) + \mathcal{O}(\varepsilon^2) \tag{5}$$

Non-dimensional thrust acceleration parameters have been introduced as $\varepsilon_x = a_T^x/(\mu/a_{ref}^2)$. The reference orbit, characterized by $\boldsymbol{\alpha}_{ref}$, is slightly different from the initial orbital elements and its value is obtained from the averaging procedure. Introducing the expansion for $\boldsymbol{\alpha}(E)$ into the ODE system for $\boldsymbol{\alpha}$ as function of E, $\mathrm{d}\boldsymbol{\alpha}/\mathrm{d}E$, differential equations for $\boldsymbol{\alpha}^t$ and $\boldsymbol{\alpha}^n$ are obtained. The solutions for $\boldsymbol{\alpha}^t$ and $\boldsymbol{\alpha}^n$ fall into three categories:

1. Elements i^t, Ω^t, a^n, i^n and Ω^n are unaffected by the corresponding thrust component.
2. Elements ω^t and e^n have only oscillatory behaviours, and their expressions can be integrated directly.
3. Elements a^t, e^t and ω^n combine secular behaviours, with time scale proportional to the thrust magnitude, and oscillatory components with period linked to the orbital one.

In general, the evolution of the elements in the last category can be expressed as:

$$\Delta\alpha = \alpha_{ref} + \varepsilon K_\alpha \Delta E + \alpha_{osc}(E)|_{E_0}^{E} \tag{6}$$

The slopes of the secular component K_α depend on a_{ref}, e_{ref}, and they contain complete elliptic integrals of the first and second kind involving only e_{ref}. The oscillatory components, instead, are obtained as a series expansion in small e_{ref}:

$$\alpha_{osc}(E) = \sum_u e_{ref}^u \sum_v^{f(u)} M_{uv}^\alpha \sin vE \tag{7}$$

where M_{uv}^α is a matrix of constant coefficients. The expressions for K_α and the numerical values for M_{uv}^α can be found in [6][16][9][10].

Plugging these results into the differential time law $\mathrm{d}t/\mathrm{d}E$, expanding in ε_x and e_{ref} up to the same orders as for $\boldsymbol{\alpha}$, and integrating yields:

$$\begin{aligned}\Delta t\, n_{ref} = \left[E - e_{ref}\,\sin E\right] + \varepsilon_t \Delta t^t\left(E; a_{ref}, e_{ref}\right) \\ + \varepsilon_n \Delta t^n\left(E; a_{ref}, e_{ref}\right) + \mathcal{O}(\varepsilon^2)\end{aligned} \tag{8}$$

where $n_{ref} = \left(\mu/a_{ref}^3\right)^{1/2}$ is the mean motion of the reference orbit, and the first term of the right-hand side corresponds to the derivative of Kepler's equation (i.e., the unperturbed case). The expressions of Δt^t and Δt^n are qualitatively analogous to those of $\Delta\alpha$ in Eq. (6), with the exception that Δt^t also includes a quadratic term in E. This indicates that the validity of the expansion for Δt will break faster than those for the Keplerian elements.

For a given CA, the change in phasing due to a CAM is obtained by solving implicit the time law $E(TCA)$ from Eq. (8), and then evaluating the updated Keplerian elements function of E. If the manoeuvre ends at a time $t_f < TCA$, the time law will be solved for this time, and the rest of the arc will be ballistic. This implicit time law has to be solved numerically, preventing the method from being entirely analytical. Instead, parametric analyses for manoeuvre duration and location in terms of anomaly can be performed without inverting the time law.

The single-averaged low-thrust CAM model allows one to evaluate the outcome of a pre-defined CAM without a numerical integration, but to optimize the CAM according to some figure of merit it should be used within an iterative numerical optimizer. A more computationally efficient approach is proposed leveraging the impulsive CAM model in Section 3.1. As previously indicated, this model reduces to an eigenproblem both for the maximum miss distance and minimum PoC problems. Then, a piecewise-constant low-thrust CAM can be defined by dividing the thrust arc in segments and assigning to each of them the orientation of the impulsive CAM at its middle point. Furthermore, it can be proven that the eigenvalue of the impulsive CAM at each segment serves as proxy for the local efficiency of the CAM compared to the other segments, which allows to construct a bang-bang structure for the control profile (as expected for minimum fuel solutions).

4. Test cases

The high computational performance of the models presented in Section 3 makes them suitable to carry out sensitivity analyses, characterizing the influence of the main parameters in the CAM design (e.g., manoeuvre timing, thrust acceleration, level of uncertainties). The results from this analysis can be expressed as maps showing the evolution of the CAM outcomes (e.g., miss distance, PoC) as function of the selected parameters. In this section some examples on different orbital regions are provided.

The first example corresponds to a low-thrust CAM in the LEO region. The manoeuvre is composed by a single tangential thrust arc, with fixed acceleration magnitude and different durations of the thrust arc, Δt_{CAM}, and of the coast arc before the CA, Δt_{coast}. The Keplerian elements at TCA of spacecraft and debris are $\boldsymbol{\alpha}_{sc}$ = [6901.4 km, 0.0017, 53.07 deg, 122.01 deg, 92.00 deg, 209.76 deg] and $\boldsymbol{\alpha}_{deb}$ = [6965.1 km, 0.0100, 124.77 deg, 297.89 deg, 275.91 deg, 320.75 deg], respectively, and the components of the combined covariance in the encounter plane are $\sigma_\xi = 0.0165$ km, $\sigma_\zeta = 0.0170$ km, and $\rho_{\xi\zeta} = 0.0160$. The evolution of miss distance δb and PoC is shown in Fig. 2 for a thrust acceleration of $a_T = 10^{-8}\ \mathrm{km/s^2}$, and in Fig. 3 for a thrust acceleration of $a_T = 10^{-9}\ \mathrm{km/s^2}$. It is observed that the CAM is feasible for both acceleration levels, but for the lower one it cannot be completed within one orbital revolution. In practice, this will require combining several thrust and coast arcs, having a significant impact in the nominal operations of the spacecraft. A feature surfacing for both thrust levels are the oscillatory patterns linked to the position of the start and end of the thrust arc along the orbit.

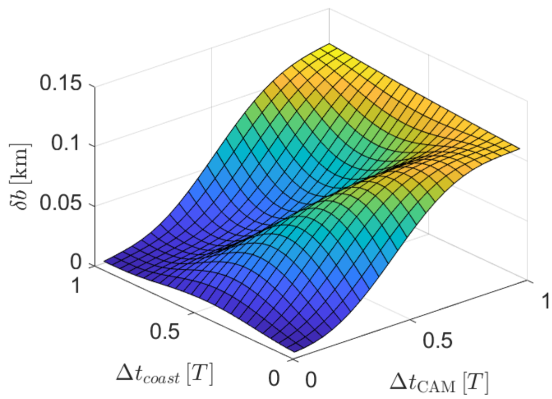

(a) Miss distance

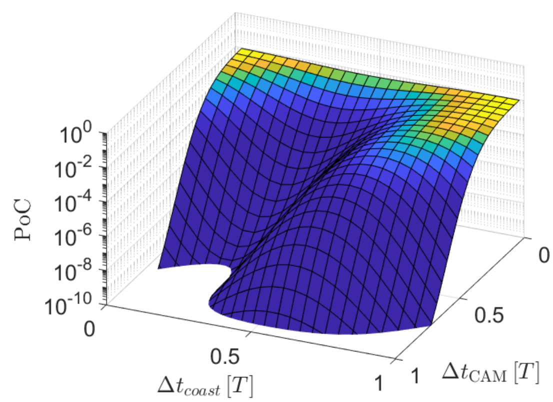

(b) Probability of collision

Fig. 2. Miss distance and PoC for a LEO test case with $a_T = 10^{-8}$ km/s^2

The next test case corresponds to a CA in the MEO region. Again, the CAM will be defined as a single, constant tangential thrust arc with duration Δt_{CAM}, and the thrusters will switch off a time Δt_{coast} before the CA. The Keplerian elements at TCA of spacecraft and debris are $\boldsymbol{\alpha}_{sc}$ = [14447.1 km, 0.0001, 0.13 deg, 69.16 deg, 329.70 deg, 245.42 deg] and $\boldsymbol{\alpha}_{deb}$ = [22647.1 km, 0.7000, 7.00 deg, 103.67 deg, 73.94 deg, 24.53 deg], respectively, and the components of the combined covariance in the encounter plane are $\sigma_\xi = 0.0594$ km, $\sigma_\zeta = 0.1521$ km, and $\rho_{\xi\zeta} = -0.1908$. The evolution of miss distance δb and PoC is shown in Fig. 4 for a thrust acceleration of $a_T = 10^{-9}$ km/s^2, and Fig. 5 for a thrust acceleration of $a_T = 10^{-10}$ km/s^2. As expected, the achievable deflection per orbit is higher than that of the LEO case, both due to the longer period and to the higher value of the non-dimensional thrust parameter ε. Indeed, ε is defined as the ratio between thrust acceleration and the local gravity acceleration (which decreases with altitude), showing that control authority grows as we move farther away from the Earth. Similarly, the oscillatory behaviours associated to the phasing of the manoeuvre are significantly softer, although still noticeable for the higher value of thrust acceleration.

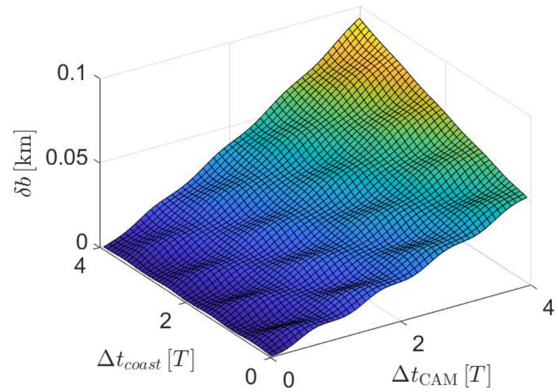

(a) Miss distance

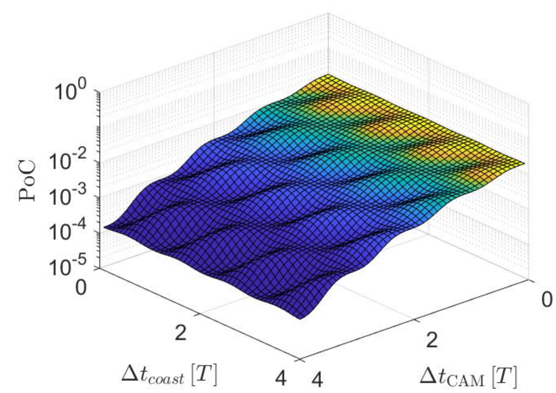

(b) Probability of collision

Fig. 3. Miss distance and PoC for a LEO test case with $a_T = 10^{-9}$ km/s^2

5. Applications for CAM mappings: ML and autonomy

The previous results show the high performance of the analytical and semi-analytical models in characterizing a set of CAs, by running sensitivity analyses on different design parameters with a limited computational cost. This already has straightforward applications as a support tool for ground operations and as initial guess generator for high-accuracy numerical resolution methods. But it can also be an enabler for more advanced techniques, such as artificial intelligence and machine learning applications, and on-board autonomy.

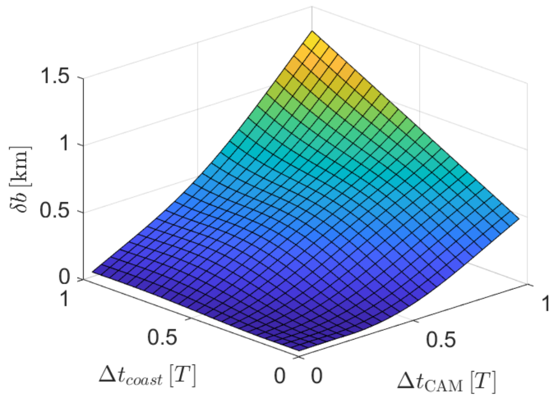

(a) Miss distance

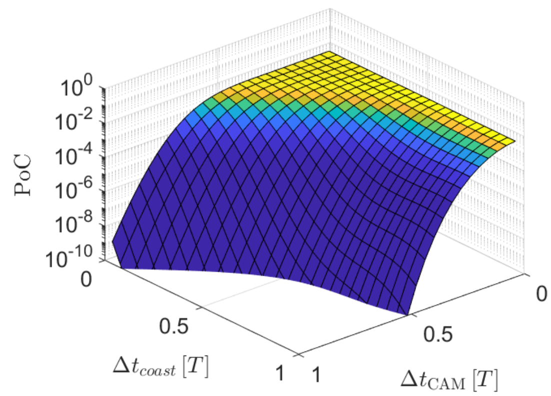

(b) Probability of collision

Fig. 4. Miss distance and PoC for a MEO test case with $a_T = 10^{-9}$ km/s^2

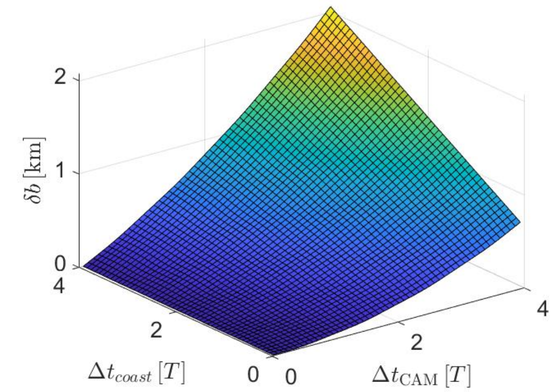

(a) Miss distance

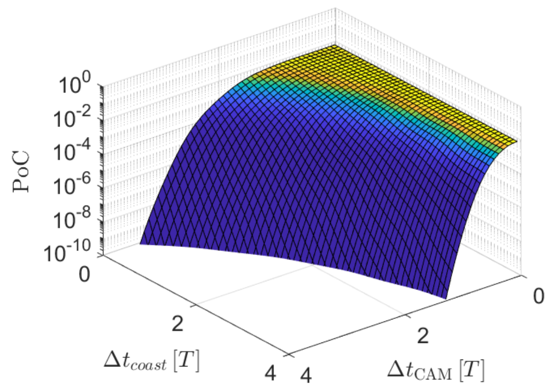

(b) Probability of collision

Fig. 5. Miss distance and PoC for a MEO test case with $a_T = 10^{-10}$ km/s^2

There are several ongoing activities to increase the level of automation in COLA activities [18], such as the AUTOCA project [19] or ESA's CREAM initiative [20]. This higher level of automation can be introduced both for ground operations, and by providing certain level of on-board autonomy. However, there is a key challenge in the limited amount of real-world data available, particularly in what regards high-risk scenarios; this was made evident by the outcomes from ESA's collision avoidance challenge in 2019 [21]. One way to address this is to generate synthetic datasets from numeric simulations. Large-scale maps like the ones enabled by (semi-)analytical CAM models can be used as training datasets for machine learning models, or to define surrogate models (e.g., fittings or lookup tables).

6. Conclusions

Analytical and semi-analytical approaches provide fast and robust tools for preliminary CAM analyses. In this work, a family of models for impulsive and low-thrust CAMs, based on Gauss planetary equations, have been leveraged to carry out parametric analyses on different CAM scenarios. For the impulsive model, the mapping between the delta-v due to the CAM and the modification of the Keplerian elements takes a simple matrix form, directly derived from Gauss planetary equations. For the low-thrust case, instead, the tangential and normal components of the thrust acceleration are decoupled under the assumption of small thrust magnitude, and their analytical solutions are obtained averaging Gauss's planetary equations one revolution in eccentric anomaly. The results are formed by a linear secular term, involving complete elliptic integrals of the first and second kinds, and oscillatory short-periodic terms. Methodologies for deriving optimal and quasi-optimal control profiles are also presented, leveraging the reduction of the optimal impulsive CAM problem to an eigenproblem.

These models have been used to carry out sensitivity analyses for different types of CAM. The influence of different parameters has been analysed, such as the timing of the manoeuvre, acceleration level, and uncertainty. The resulting maps can be enablers for other applications, such as the training of machine learning algorithms.

Acknowledgements

This work has received funding from the European Space Agency through the project "ELECTROCAM: Assessment of collision avoidance manoeuvre planning for low-thrust missions" (call AO/1-10666/21/D/SR). It has also received funding from the European Research Council (ERC) under the European Union’s Horizon 2020 research and innovation programme (grant agreement No 679086 – COMPASS).

Juan Luis Gonzalo also thanks the funding of his research position by the Italian Ministero dell’Università e della Rierca, Programma Operativo Nazionale (PON) “Ricerca e Innovazione” 2014-2020, contract RTDA – DM 1062 (REACT-EU).

References

[1] C. Bombardelli, and J. Hernando Ayuso, Optimal Impulsive Collision Avoidance in Low Earth Orbit, Journal of Guidance, Control, and Dynamics, 38, 2 (2015), 217-225. https://doi.org/10.2514/1.G000742

[2] J. Hernando Ayuso, and C. Bombardelli, Low-Thrust Collision Avoidance in Circular Orbits, Journal of Guidance, Control, and Dynamics, 44, 5 (2021), 983-995. https://doi.org/10.2514/1.G005547

[3] C. Colombo, A. De Vittori, M. Omodei, J.L. Gonzalo, M. Maestrini, P. Di Lizia, P. Gago Padreny, M. Torras Ribell, A. Gallego Torrego, D. Escobar Antón, and Roberto Armellin, Sensitivity analysis of collision avoidance manoeuvre with low thrust propulsion, Aerospace Europe Conference 2023 (10th EUCASS - 9th CEAS), Lausanne, Switzerland, 2023, 9-13 July.

[4] M. Maestrini, A. De Vittori, P. Di Lizia, and C. Colombo, Dynamics-Based Uncertainty Propagation with Low-Thrust, 2022 AAS/AIAA Astrodynamics Specialist Conference, Charlotte, NC, USA, 2022, 7-11 August.

[5] M. Maestrini, A. De Vittori, J.L. Gonzalo, C. Colombo, P. Di Lizia, J. Míguez Arenas, M. Sanjurjo Rivo, A. Diez Martín, P. Gago Padreny, and D. Escobar Antón, ELECTROCAM: Assessing the Effect of Low-Thrust Uncertainties on Orbit Propagation, 2nd ESA NEO and debris detection conference, Darmstadt, Germany, 2023, 24-26 January.

[6] J.L. Gonzalo, C. Colombo, and P. Di Lizia, Single-averaged models for low-thrust collision avoidance under uncertainties, 73rd International Astronautical Congress, Paris, France, 2022, 18-22 September.

[7] J.L. Gonzalo, C. Colombo, and P. Di Lizia, Introducing MISS, a new tool for collision avoidance analysis and design, Journal of Space Safety Engineering, 7, 3 (2020) 282–289. https://doi.org/10.1016/j.jsse.2020.07.010

[8] J.L. Gonzalo, C. Colombo, and P. Di Lizia, Analytical framework for space debris collision avoidance maneuver design, Journal of Guidance, Control and Dynamics, 44, 3 (2021) 469-487. https://doi.org/10.2514/1.G005398

[9] J.L. Gonzalo, C. Colombo, and P. Di Lizia, A semi-analytical approach to low-thrust collision avoidance manoeuvre design, 70th International Astronautical Congress, Washington, D.C., USA, 2009, 21–25 October. Paper number IAC-19-A6.2.3

[10] J.L. Gonzalo, C. Colombo, and P. Di Lizia, Computationally Efficient Approaches for Low-Thrust Collision Avoidance Activities, 72nd International Astronautical Congress, Dubai, UAE, 2021, 25-29 October. Paper number IAC-21-A6.10-B6.5.5.

[11] Y. Gao, Near-optimal very low-thrust earth-orbit transfers and guidance schemes, Journal of Guidance Control and Dynamics, 30, 2 (2017), 529-539.

[12] J. L. Junkins, and H. Schaub, Analytical mechanics of space systems. American Institute of Aeronautics and Astronautics, Reston, VA, 2009.

[13] F. K. Chan, Spacecraft Collision Probability, Aerospace Press, 2008, Chap. 6.

[14] R. H. Battin, An introduction to the mathematics and methods of Astrodynamics, AIAA Education series, AIAA, Reston, VA, 1999.

[15] M. Vasile, and C. Colombo, Optimal Impact Strategies for Asteroid Deflection, Journal of Guidance, Control, and Dynamics, 31, 4 (2008) 858–872. https://doi.org/10.2514/1.33432

[16] J.L. Gonzalo, and C. Colombo, Lightweight algorithms for collision avoidance applications, 11th ESA GNC, virtual conference, 2021, 22-25 June.

[17] B. Conway, Near-Optimal Deflection of Earth-Approaching Asteroids, Journal of Guidance, Control, and Dynamics, 24, 5 (2001), 1035–1037. https://doi.org/10.2514/2.4814

[18] M. Vasile, V. Rodriguez-Fernandez, R. Serra, D. Camacho, and A. Riccardi, Artificial Intelligence in Support to Space Traffic Management, 68th International Astronautical Congress, Adelaide, Australia, 2017, 25–29 September.

[19] "AUTOCA Autonomous Collision Avoidance System for NGSO", https://artes.esa.int/projects/autoca [accessed 01/09/2023]
[20] B. Bastida Virgili, T. Flohrer, H. Krag, K. Merz, and S. Lemmens, CREAM - ESA's Proposal for Collision Risk Estimation and Automated Mitigation. First International Orbital Debris Conference (IOC), Sugarland (TX), US, 2019, 9-12 December. Paper 6031.
[21] T. Uriot, et al., Spacecraft collision avoidance challenge: Design and results of a machine learning competition, Astrodynamics, 2021. https://doi.org/10.1007/s42064-021-0101-5